Proinsulin Slows Retinal Degeneration and Vision Loss in the P23H Rat Model of Retinitis Pigmentosa

Laura Fernández-Sánchez,[1,*] Pedro Lax,[1,*] Carolina Isiegas,[2] Eduard Ayuso,[3] José M. Ruiz,[2]
Pedro de la Villa,[4] Fatima Bosch,[3] Enrique J. de la Rosa,[5] and Nicolás Cuenca[1,6]

Abstract

Proinsulin has been characterized as a neuroprotective molecule. In this work we assess the therapeutic potential of proinsulin on photoreceptor degeneration, synaptic connectivity, and functional activity of the retina in the transgenic P23H rat, an animal model of autosomal dominant retinitis pigmentosa (RP). P23H homozygous rats received an intramuscular injection of an adeno-associated viral vector serotype 1 (AAV1) expressing human proinsulin (hPi+) or AAV1-null vector (hPi−) at P20. Levels of hPi in serum were determined by enzyme-linked immunosorbent assay (ELISA), and visual function was evaluated by electroretinographic (ERG) recording at P30, P60, P90, and P120. Preservation of retinal structure was assessed by immunohistochemistry at P120. Human proinsulin was detected in serum from rats injected with hPi+ at all times tested, with average hPi levels ranging from 1.1 nM (P30) to 1.4 nM (P120). ERG recordings showed an amelioration of vision loss in hPi+ animals. The scotopic b-waves were significantly higher in hPi+ animals than in control rats at P90 and P120. This attenuation of visual deterioration correlated with a delay in photoreceptor degeneration and the preservation of retinal cytoarchitecture. hPi+ animals had 48.7% more photoreceptors than control animals. Presynaptic and postsynaptic elements, as well as the synaptic contacts between photoreceptors and bipolar or horizontal cells, were preserved in hPi+ P23H rats. Furthermore, in hPi+ rat retinas the number of rod bipolar cell bodies was greater than in control rats. Our data demonstrate that hPi expression preserves cone and rod structure and function, together with their contacts with postsynaptic neurons, in the P23H rat. These data strongly support the further development of proinsulin-based therapy to counteract retinitis pigmentosa.

Introduction

RETINITIS PIGMENTOSA (RP) CONSTITUTES a large heterogeneous group of inherited neurodegenerative retinal disorders that cause a progressive loss of retinal function and represent a major cause of blindness. More than 100 different mutations in the rhodopsin-encoding gene (*RHO*) are associated with RP, together accounting for 30% to 40% of autosomal dominant cases. The P23H mutation in *RHO* is the most prevalent cause of RP (Dryja *et al.*, 1990), which alone accounts for approximately 12% of autosomal dominant RP cases in the United States (Dryja *et al.*, 2000). The majority of RP-causing mutations in the *RHO* gene, including P23H, cause misfolding and retention of rhodopsin in the endoplasmic reticulum of transfected cultured cells (Kaushal and Khorana, 1994). These studies also suggest that the mechanism of RP involves a cellular stress response (Illing *et al.*, 2002), the final common pathway being programmed photoreceptor cell death by apoptosis (Reme *et al.*, 1998). P23H transgenic albino rats suffer from a progressive retinal degeneration, which is consistent with the clinical findings in P23H patients (Berson *et al.*, 1991; Cuenca *et al.*, 2004; Machida *et al.*, 2000; Pinilla *et al.*, 2005). The loss of photoreceptors is accompanied by degenerative changes in the inner retina (Cuenca *et al.*, 2004;

[1]Department of Physiology, Genetics and Microbiology, University of Alicante, E-03080 Alicante, Spain.
[2]ProRetina Therapeutics SL, Centro de Investigaciones Biologicas and CEIN, E-28040 Madrid and E-31110 Noain, Spain.
[3]Center of Animal Biotechnology and Gene Therapy and Department of Biochemistry and Molecular Biology, School of Veterinary Medicine, Universitat Autònoma de Barcelona, E-08193 Bellaterra, Spain.
[4]Department of Physiology, School of Medicine, University of Alcalá, Alcalá de Henares, E-28801 Madrid, Spain.
[5]3D Lab (Development, Differentiation and Degeneration), Department of Cellular and Molecular Medicine, Centro de Investigaciones Biológicas, Consejo Superior de Investigaciones Científicas, 28040 Madrid, Spain.
[6]Multidisciplinary Institute for Environmental Studies "Ramon Margalef", University of Alicante, E-03080 Alicante, Spain.
*These authors contributed equally to this work.

Marc *et al.*, 2003; Puthussery and Taylor, 2010), and a substantial degeneration of retinal ganglion cells (Jones *et al.*, 2003; Kolomiets *et al.*, 2010).

Several strategies are being investigated to slow or cure this group of diseases. Gene therapy, encapsulated cells releasing neurotrophic factors, and stem cell transplantation are hopeful future approaches to RP treatment (Musarella and Mac-Donald, 2011). Today, gene therapy for RP has been successfully used in animal models (Chadderton *et al.*, 2009; Millington-Ward *et al.*, 2011; Palfi *et al.*, 2010; Pang *et al.*, 2011; Pinilla *et al.*, 2007, 2009) and humans (Bainbridge *et al.*, 2008; Maguire *et al.*, 2008, 2009). However, therapy for P23H rhodopsin-induced RP represents a challenge because of its autosomal dominant nature (Farrar *et al.*, 2010). Molecules that promote survival, such as brain-derived neurotrophic factor, ciliary neurotrophic factor, fibroblast growth factor, glial-derived neurotrophic factor, and pigment epithelium-derived factor, are moderately successful in preventing disease progression when used in animal models (Cayouette *et al.*, 1998, 1999; Chong *et al.*, 1999; Green *et al.*, 2001; McGee Sanftner *et al.*, 2001; Okoye *et al.*, 2003). Antioxidants also provide modest retinal protection in animal models of RP, probably by reducing oxidative damage (Ahuja *et al.*, 2005; Berson *et al.*, 1993; Komeima *et al.*, 2006; Lax *et al.*, 2011). Finally, attenuation of apoptosis represents a good therapeutic target in RP, especially considering the vast heterogeneity of the disease (Doonan and Cotter, 2004; Lax *et al.*, 2011; Liang *et al.*, 2001). In that sense, tauroursodeoxycholic acid, a component of bear bile, has been shown to exhibit antiapoptotic properties in neurodegenerative diseases and the capacity to preserve cone and rod structure and function together with their contacts with postsynaptic neurons (Boatright *et al.*, 2006, 2009; Fernandez-Sanchez *et al.*, 2011; Phillips *et al.*, 2008).

Proinsulin, a member of the insulin superfamily, has been characterized as a neuroprotective molecule that is active in development and aging (de la Rosa and de Pablo, 2011; de Pablo and de la Rosa, 1995; Vergara *et al.*, 2012). During embryonic retinal development, proinsulin acts as a survival factor in chick and mouse (Diaz *et al.*, 2000; Duenker *et al.*, 2005; Hernandez-Sanchez *et al.*, 1995; Valenciano *et al.*, 2006). Conversely, treatment with exogenous proinsulin *in ovo* results in a reduction of naturally occurring apoptosis (Hernandez-Sanchez *et al.*, 2003), and experimentally induced cell death in the developing retina is prevented by proinsulin (Diaz *et al.*, 2000). In the rod-specific insulin receptor (InsR) knockout mouse, increased sensitivity to light-induced photoreceptor degeneration was observed, providing direct evidence of a functional role for the InsR in photoreceptor cell survival (Rajala *et al.*, 2008). Finally, transgenic expression of human proinsulin in skeletal muscle in the rd10 mouse model of RP attenuated retinal degeneration, as assessed by the maintenance of electroretinographic (ERG) responses and the histological preservation of photoreceptors (Corrochano *et al.*, 2008). Systemic proinsulin was able to reach retinal tissue, delay apoptotic death of photoreceptors, and decrease oxidative damage. Thus, proinsulin represents a potential new therapy for RP and a new tool to characterize the mechanisms involved in pathologic cell death. Here we assess the therapeutic potential of proinsulin on photoreceptor degeneration, synaptic connectivity, and functional activity of the retina in the transgenic P23H rat using adeno-associated vector (AAV)-mediated expression.

Materials and Methods

Animals

Homozygous P23H (line 3) albino rats, obtained from Dr. M. LaVail (UCSF School of Medicine; www.ucsfeye.net/mlavailRDratmodels.shtml), were used in this study. All animals were bred in a colony at the Universidad de Alicante and maintained under controlled humidity (60%), temperature ($23 \pm 1°C$), and photoperiod (light:dark 12:12) conditions. All animals were handled in accordance with current regulations for the use of laboratory animals (National Institutes of Health, Association for Research in Vision and Ophthalmology, and the European Directive 86/609/EEC) in order to minimize animal suffering and numbers used for experiments.

AAV vector production and administration

Vectors were generated by triple transfection method in human embryonic kidney 293 cells according to standard protocols (Matsushita *et al.*, 1998). Cells were cultured to 80% confluence in roller bottles (Corning, New York, NY) in Dulbecco's modified Eagle's medium 10% fetal bovine serum and co-transfected using the calcium phosphate method. Expression of the human proinsulin cDNA was driven by the cytomegalovirus promoter. AAV-null vectors are noncoding vectors and were produced using pAAV-MCS plasmid (Stratagene, La Jolla, CA). AAVs were purified with an optimized method based on a polyethylene glycol precipitation step and two consecutive cesium chloride (CsCl) gradients (Ayuso *et al.*, 2010). Purified AAV vectors were dialyzed against phosphate-buffered saline, filtered, and stored at $-80°C$. Titers of viral genomes were determined by quantitative PCR following the protocol described for the AAV2 Reference Standard Material (Lock *et al.*, 2010).

An adeno-associated viral vector serotype 1 (AAV1) expressing human proinsulin (hPi+) was injected intramuscularly at a dose of 10^{13} vector genomes/kg to P23H rats at P20. The total dose of vectors was distributed in quadriceps, gastrocnemius, and tibialis cranialis muscles of both hind limbs. Control animals received the same doses of AAV1-null vector (hPi−).

ERG recordings

Scotopic and photopic ERGs were performed at P30, P60, P90, and P120. Following overnight dark adaptation, animals were prepared for bilateral ERG recording under dim red light. Animals were anesthetized by intraperitoneal injection of a ketamine (100 mg/kg; Imalgene®, Merial Laboratorios S.A., Barcelona, Spain) plus xylazine (4 mg/kg; Xilagesic 2%, Laboratorios Calier, Barcelona, Spain) solution, and maintained on a heated pad at 38°C. Pupils were dilated by topical application of 1% tropicamide (Alcon Cusí, Barcelona, Spain). A drop of Viscotears 0.2% polyacrylic acid carbomer (Novartis, Barcelona, Spain) was instilled on the cornea to prevent dehydration and allow electrical contact with the recording electrodes (DTL fiber electrodes with an X-Static silver-coated nylon conductive yarn; Sauquoit Industries, Scranton, PA). A 25-gauge platinum needle inserted under the scalp between the two eyes served as the reference electrode. A gold electrode was placed in the mouth and served as ground. Anesthetized animals were placed on a

Faraday cage and all experiments were performed in absolute darkness. Scotopic flash-induced ERG responses were recorded from both eyes in response to light stimuli produced by a Ganzfeld stimulator. Light stimuli were presented for 10 msec at 11 different increasing intensities (ranging from −5.7 to 0 log cd·sec/m^2). Three to 10 consecutive recordings were averaged for each light presentation. The interval between light flashes was 10 sec for dim flashes and up to 20 sec for the highest intensity. Photopic responses were obtained after light adaptation at 10 cd/m^2 during 20 min, and stimuli were the same as for scotopic conditions. The ERG signals were amplified and band-pass filtered (1 to 1000 Hz, without notch filtering) using a DAM50 data acquisition board (World Precision Instruments, Aston, UK). Stimulus presentation and data acquisition (4 kHz) were performed using a PowerLab system (ADInstruments, Oxfordshire, UK). Recordings were saved on a computer and analyzed off-line. The amplitude of the a-wave was measured from the baseline to the trough of the a-wave, and the results were averaged. The amplitude of the b-wave was measured from the trough of the a-wave to the peak of the b-wave and averaged for different recordings. For both scotopic and photopic intensity-response curves, thresholds were defined as the minimal luminance required to reach the criterion amplitude of 10 μV.

Detection of serum proinsulin and glycemia

Blood samples were taken at P20, P30, P60, P90, and P120 to determine proinsulin levels in serum and glycemia. To obtain the serum, blood was collected in anticoagulant-free tubes, kept at room temperature until clot formation (around 30 min) and then centrifuged (2000×g, 15 min at 4°C). Serum was transferred to tubes that were flash-frozen and then stored at −20°C until analysis. The levels of human proinsulin in serum were measured using the Human Total Proinsulin enzyme-linked immunosorbent assay (ELISA) kit (Merck Millipore, Darmstadt, Germany) following manufacturer's instructions. Glycemia was measured *in situ* by the Glucocart™ Gmeter kit (A. Menarini Diagnostics Ltd., Berkshire, UK).

Retinal histology

Retinal sections. Animals were sacrificed upon administration of a lethal dose of pentobarbital, and their eyes were enucleated, fixed in 4% paraformaldehyde, and sequentially cryoprotected in 15%, 20%, and 30% sucrose. After being washed in 0.1 M phosphate buffer (PB) pH 7.4, the cornea, lens, and vitreous body were removed, and the retinas were processed for vertical sections. For this purpose, they were embedded in OCT and frozen in liquid N$_2$. Sixteen-micrometer-thick sections were then obtained at −25°C, mounted on Superfrost Plus slides (Menzel GmbH & Co KG, Braunschweig, Germany), and air-dried. Before further use, slides were thawed and washed three times in PB, and then treated with blocking solution (10% normal donkey serum in PB plus 0.5% Triton X-100) for 1 hr at room temperature.

Retinal immunohistochemistry. For objective comparison, retinas from hPi+ and hPi− rats were fully processed in parallel. Primary antibodies used in this work are summarized in Table 1. Sections were subjected to single or double

TABLE 1. PRIMARY ANTIBODIES

Molecular marker	Antibody	Source	Dilution
Calbindin D-28K	Rabbit polyclonal	Swant	1:500
Protein kinase C, alpha isoform	Rabbit polyclonal	Santa Cruz Biotechnology	1:100
Bassoon	Mouse monoclonal	Stressgen	1:1000

immunostaining overnight at room temperature with combinations of antibodies for different molecular markers at the dilutions indicated in Table 1, in PB containing 0.5% Triton X-100. Subsequently, Alexa Fluor 488 (green)–conjugated anti-rabbit IgG and/or Alexa Fluor 555 (red)–conjugated anti-mouse IgG donkey secondary antibodies from Molecular Probes (Eugene, OR) were applied at a 1:100 dilution for 1 hr. The sections were finally washed in PB, mounted in Citifluor (Citifluor Ltd., London, UK) and coverslips applied for viewing under laser-scanning confocal microscopy on a Leica TCS SP2 system (Leica Microsystems, Wetzlar, Germany). Immunohistochemical controls were performed by omission of either the primary or secondary antibodies. Final images from control and experimental subjects were processed in parallel using the Adobe Photoshop 10 software (Adobe Systems Inc., San José, CA).

Retinal layer thickness. Animals were examined for measurements of the outer nuclear layer (ONL) thickness, using the nuclear stain TO-PRO-3 iodide (Molecular Probes) added at a 1:1000 dilution, in at least two sections from each animal containing the optic nerve and both temporal and nasal orae serratae. Counting of photoreceptor rows was performed at distances of 0.5, 1.5, 2.5, and 3.5 mm from the optic nerve toward each ora serrata. Quantifications were done in a blinded fashion by multiple experienced observers.

Statistical analyses

Statistical analyses were performed using SPSS 15.0 software (IBM, Armonk, NY). A repeated measures factorial analysis of variance (ANOVA) was performed to evaluate the effects of treatment (hPi+ vs. hPi−) on ERG responses throughout the experimental stages (P30, P60, P90, and P120), as well as the interactions among them. When a 0.05 level of significance was found, *post hoc* pairwise comparisons using Bonferroni's test were performed. Normal distributions and homogeneity of variance were found for all the analyzed categories. A paired Student's *t*-test was used when only two groups were compared. A regression analysis was performed to establish the relationship between the maximum scotopic ERG b-wave amplitude and the mean number of rows of photoreceptor cell bodies in the ONL. P values less than 0.05 were considered statistically significant. Data were plotted as the average ± standard error of the mean (SEM).

Results

AAV-mediated proinsulin production in P23H rats

P23H rats were intramuscularly injected with AAV1-hPi or AAV1-null at P20. Human proinsulin was detected in
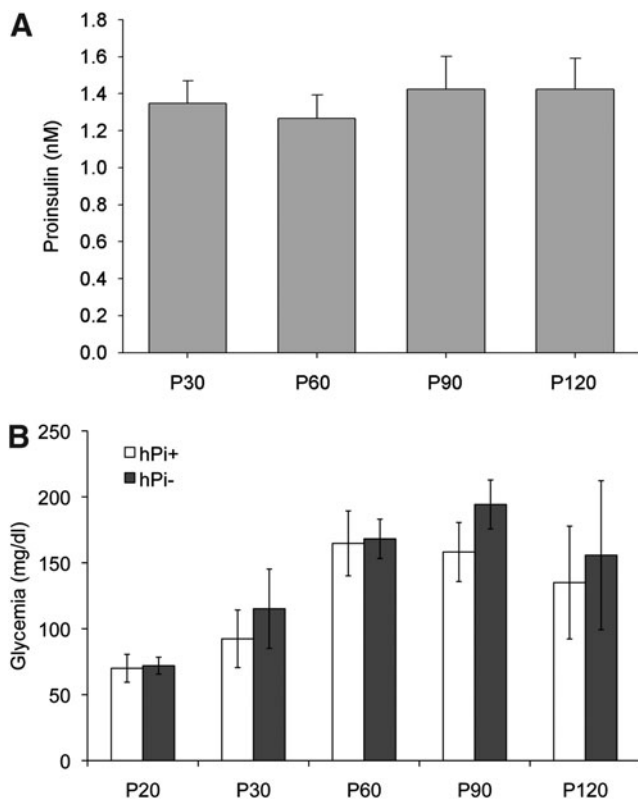
FIG. 1. Serum proinsulin and glucose measured 10, 40, 70, and 100 days after vector administration. **(A)** Serum levels of human proinsulin (hPi) measured at P30, P60, P90, and P120 in P23H rats injected with adeno-associated viral vector serotype 1 (AAV1)-hPi at P20. Note that significant expression of hPi from the viral vectors was found as early as 10 days after injection. No hPi was detected in serum from control rats (not shown). **(B)** Glycemia in hPi+ and hPi− rats measured at P20, P30, P60, P90, and P120. Error bars indicate SEM.

serum at all times tested after vector administration (Fig. 1). Average proinsulin levels ranged from $1.3 \pm 0.1\,nM$ (P30) to $1.4 \pm 0.2\,nM$ (P120). No proinsulin production was detected in hPi− rats serum (not shown). To rule out potential metabolic effects of hPi expression, blood glucose levels of hPi+ rats were compared with those of hPi− animals over the experimental period. We observed that glycemia increased over time, a phenotype that has already been described in wild-type male Sprague-Dawley rats (Petterino and Argentino-Storino, 2006). Nevertheless, no significant differences in glycemia were observed between hPi+ and hPi− animals (Student's t-test, $p = 0.11$) (Fig. 1). These results show that the AAV1 vector lead to high levels of hPi in serum, which do not affect serum glucose levels.

Proinsulin preserves retinal responsiveness

In order to evaluate the effect of proinsulin on the functional activity of the P23H rat's photoreceptors, scotopic and photopic flash-induced ERG responses were recorded in hPi+ and hPi− animals. As shown in Figure 2, ERG responsiveness was less deteriorated in hPi+ rats compared to control animals. Under scotopic conditions, the mean amplitudes recorded for b-waves were higher in hPi+ animals,

compared to values obtained in control animals, at P90 and P120 (ANOVA, Bonferroni's test, $p < 0.005$ for P90, $p < 0.001$ for P120). Thresholds in hPi+ animals, compared with control rats, were lower for scotopic b-waves (Student's t-test $p < 0.05$) at both P90 (-4.8 log cd·sec/m^2 vs. -3.9 log cd·sec/m^2) and P120 (-3.5 log cd·sec/m^2 vs. -2.6 log cd·sec/m^2). There were no significant differences in the scotopic a-waves or the photopic ERG responses between hPi+ and hPi− rats (data not shown).

### Proinsulin slows photoreceptor degeneration

To assess the protective action of proinsulin on photoreceptors, we determined in each retina the mean number of photoreceptor rows present in the ONL at P120, using the nuclear dye TO-PRO-3. Because retinal degeneration in control P23H rats was not homogeneous throughout the retina, we studied the effects of proinsulin in different retinal areas, from temporal to nasal. We found that the thickness of the ONL was higher in hPi+ ($n = 10$) than in control animals ($n = 5$) (Fig. 3; $p < 0.001$ in nasal area $P < 0.05$ in temporal and central area; Student's t-test). Proinsulin showed its best neuroprotective effect at the ONL level in the nasal area of the retina (Fig. 3), where 4-month-old hPi+ rats showed approximately 70% more rows of photoreceptor cell bodies than hPi− animals (1.49 ± 0.04 vs. 0.87 ± 0.05, respectively). The mean number of rows of photoreceptor cell bodies found in hPi+ rats positively correlated with the maximum scotopic ERG b-wave amplitude recorded for each animal at P120 ($f = y_0 + a \times x$, $R = 0.59$, $p < 0.01$; where $y_0 = $ y-intercept and $a = $ slope).

Proinsulin preserves loss of ON bipolar cells

All rod bipolar cells and a particular subtype of amacrine cells were labeled with antibodies against protein kinase C (PKC), α isoform. In the P120 retinas of hPi− rats, rod bipolar cells showed a substantial loss of cell bodies (Figs. 4A, 5A). The number of immunopositive cells appeared to decrease, and their cell bodies were not aligned in the orderly fashion found in wild-type rats (Cuenca *et al.*, 2004). In hPi+ animals, the loss of bipolar cell bodies was not as extensive (Fig. 4B, 5B). Counting of bipolar cells in retinal sections showed a greater number of immunopositive cells in the retinas of hPi+ animals ($n = 10$) compared to controls ($n = 5$). The differences were significant in the temporal side of the retina, where the degeneration was faster (Fig. 4C).

Proinsulin preserves synaptic connectivity in the outer plexiform layer

We next explored in detail whether the preservation of photoreceptors was accompanied by a preservation of synaptic connectivity in the outer plexiform layer (OPL). To this end, we used antibodies against bassoon, a protein constituent of synaptic ribbons present in both rod spherules and cone pedicles in the OPL. Typical bassoon-immunoreactive spots were observed, with the horseshoe morphology corresponding to rod spherules (Fig. 5C, 5D, arrows). Few bassoon-immunopositive spots were found at the OPL level in P120 hPi− rats (Fig. 5C), indicating a decreased number of photoreceptor axon terminals. However, hPi+ animals showed more bassoon-immunoreactive puncta (Fig. 5D), indicating that the presynaptic contact elements between
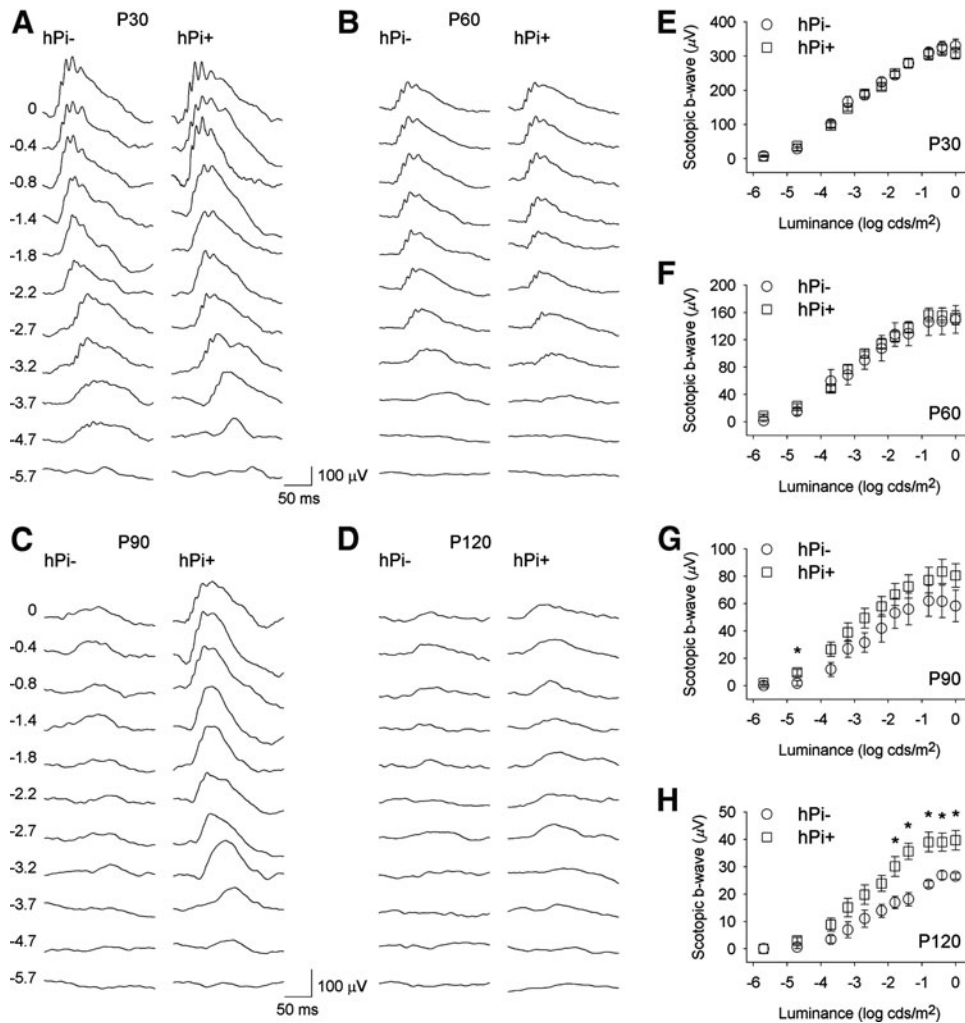
FIG. 2. Electroretinographic (ERG) responses in control (hPi−) and proinsulin expressing (hPi+) P23H rats. Representative scotopic ERG traces in a hPi− and a hPi+ rat at **(A)** P30, **(B)** P60, **(C)** P90, and **(D)** P120. Units on the left of the panels indicate input flash intensities in log cd·sec/m^2. **(E–H)** Scotopic ERG intensity-response curves of b-waves in hPi− (circle) and hPi+ (square) rats at different ages. Average amplitudes of scotopic b-waves recorded in hPi+ rats ($n=11$) were significantly higher than those observed in hPi− ($n=5$) at P90 and P120. Paired comparisons for each light stimulus showed differences between hPi+ and hPi− animals at P120. *$p < 0.05$; ANOVA, Bonferroni's test. Error bars indicate SEM.

photoreceptors and bipolar or horizontal cells were—at least partially—preserved.

Proinsulin prevents loss of ON bipolar cell dendrites and their synaptic contacts with photoreceptors

In the rat retina, dendritic terminals of ON rod bipolar cells establish connections with rod spherules through a large dendritic arbor in the OPL, and their axons run into the inner plexiform layer, each one ending in a bulbous axon terminal in the S5 stratum. In the retinas of P120 hPi− rats, rod bipolar cells showed a substantial retraction of their dendrites (Fig. 5A). Dendritic branches were scarce, and some cells were almost entirely devoid of dendrites. By contrast, in hPi+ animals, bipolar cell dendrites were preserved (Fig. 5B). Double immunostaining for bassoon and PKC showed the relationship between rod photoreceptor axon terminals and bipolar cell dendritic tips. In retinas from hPi− rats labeled at P120 with antibodies against these two markers, few bassoon-positive dots (Fig. 5E) could be seen paired with PKC-labeled bipolar cell dendrites (green). However, in hPi+ rat retinas the number of bassoon-immunoreactive spots associated with bipolar cell dendritic tips was clearly higher (Fig. 5F).

Proinsulin prevents loss of horizontal cell dendrites and their synaptic contacts with photoreceptors

Horizontal cell bodies are located in the outermost inner nuclear layer of the retina and establish connections with both rod and cone photoreceptors. The only horizontal cell subtype described in the rat retina can be identified using antibodies against calbindin. In wild-type rats, calbindin labeling revealed a punctate staining of dendritic arborization protruding from horizontal cell bodies and connecting with cone axon terminals, together with thin tangential axonal elongations in the OPL ending in an extensive arborization connecting with rods (Cuenca et al., 2004). In hPi− rats at P120, a retraction and loss of horizontal cell dendritic tips was found concomitantly with the decrease of TO-PRO-3–stained photoreceptor rows (Fig. 6A). In hPi+ rat retinas, by contrast, a higher number of horizontal cell terminals could be observed (Fig. 6B). Double labeling with antibodies against bassoon and calbindin showed numerous pairings between photoreceptor axons and horizontal cell terminals in hPi+ animals (Fig. 6E) compared with fewer contacts observed in hPi− rats (Fig. 6F). These data indicate a preserving effect of proinsulin on synaptic contacts between photoreceptors and horizontal cells.

FIG. 3. Number of photo-receptor rows in the outer nuclear layer (ONL) under hPi expression. Representative vertical sections from **(A)** hPi− and **(B)** hPi+ rat retinas at P120 stained with TO-PRO-3 iodide. Animals treated with AAV1-hPi display a higher number of photoreceptor rows at the ONL than the untreated animals. **(C)** Average number of photoreceptor rows at different distance from the optic nerve, along the naso-temporal axis. Note that preservation of photoreceptors is more significant in the nasal retina than in the temporal retina. *$p < 0.05$, **$p < 0.01$; Student's t test. Scale bar: 50 μm. Error bars indicate SEM.
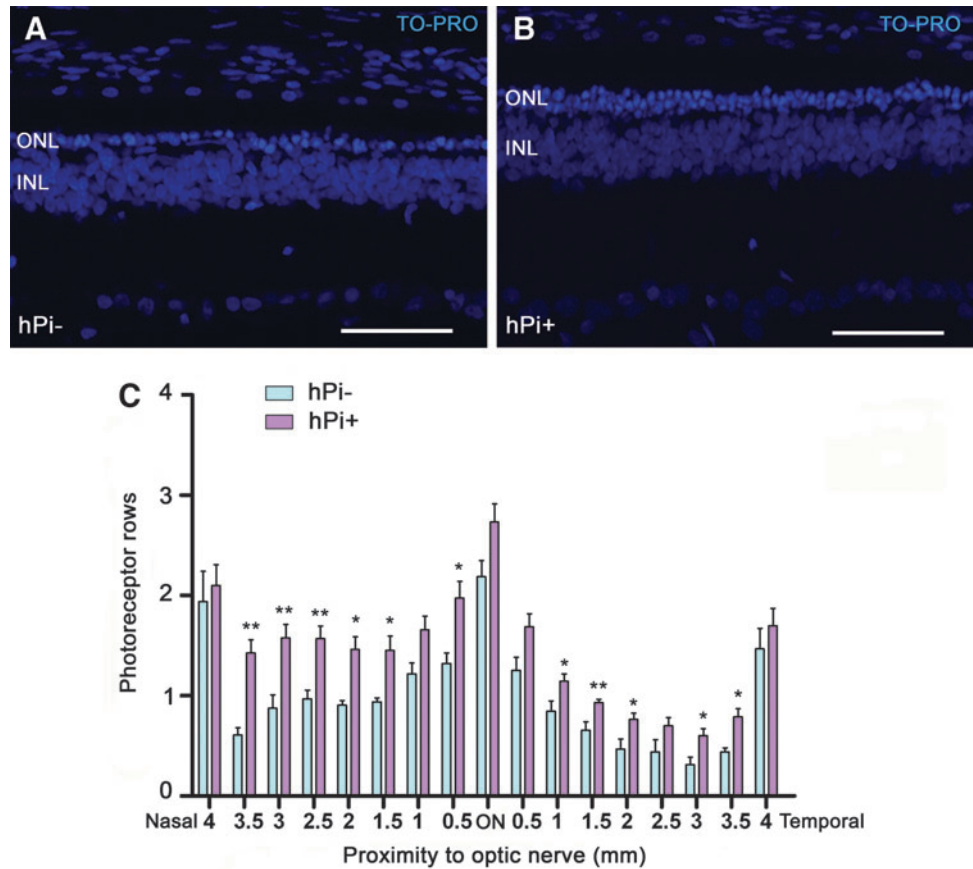
FIG. 4. Rod bipolar cells preservation by hPi. Representative vertical sections from **(A)** control and **(B)** hPi+ rat retinas at P120. **(C)** Immunostaining for protein kinase C (PKC) and quantification shows that hPi+ rats display a statistically significant higher number of bipolar cells than control hPi− in the temporal retina. *$p < 0.05$; **$p < 0.01$; ***$p < 0.001$; Student's t test. Scale bar: 50 μm. Error bars indicate SEM.
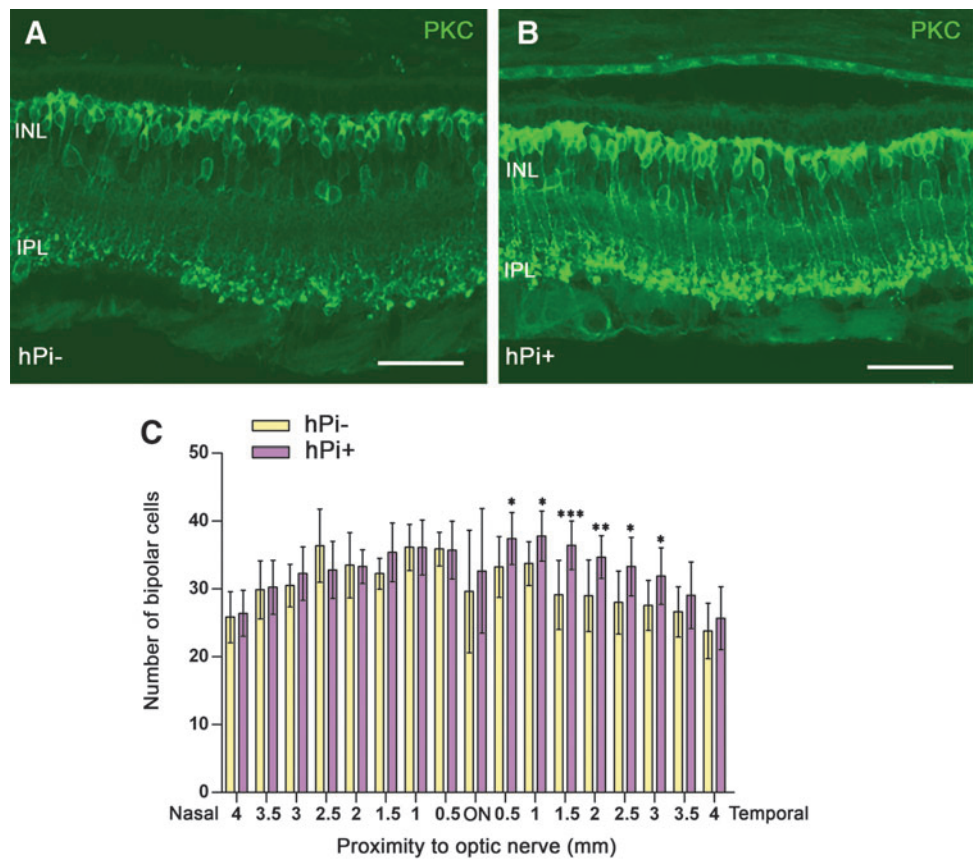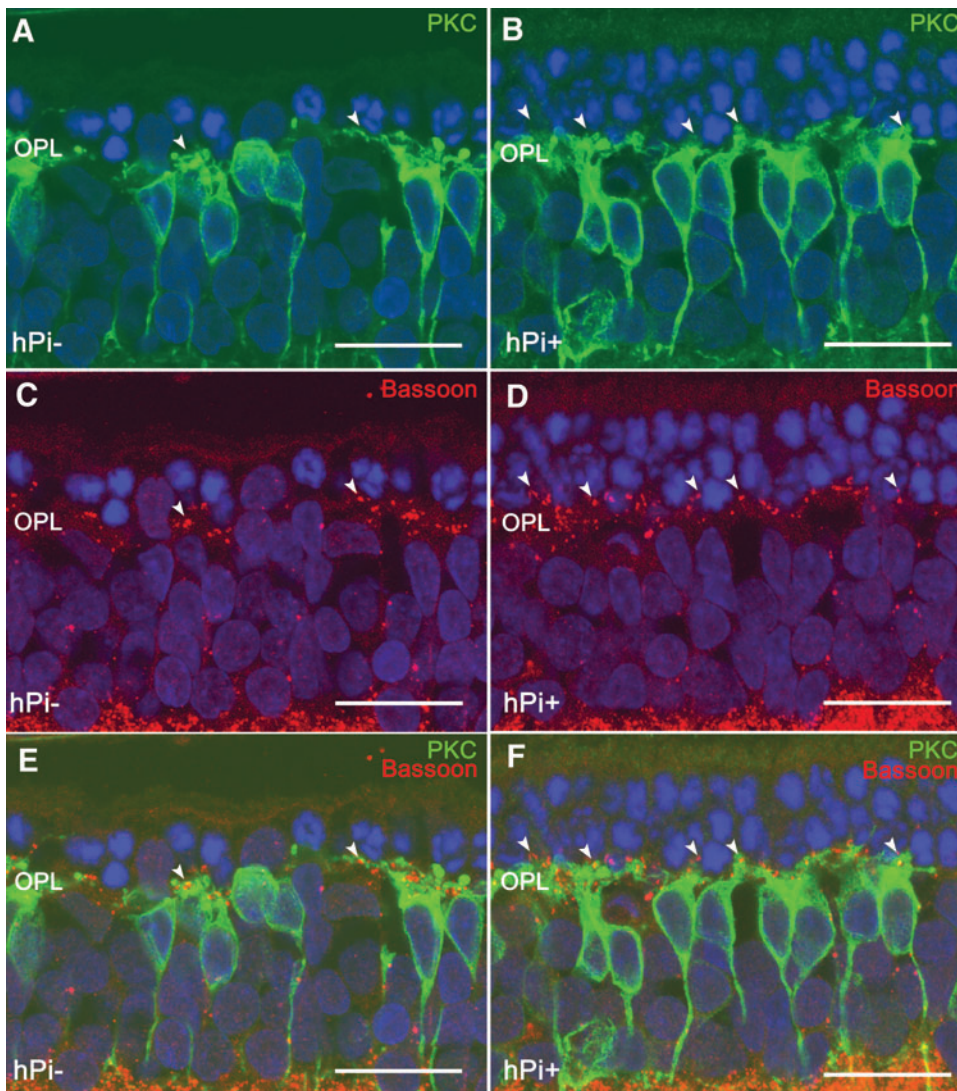
FIG. 5. Synaptic connectivity in outer plexiform layer (OPL) and rod bipolar cells in hPi− and hPi+ P23H rats. Immunostaining for PKC (*green*) and Bassoon (*red*) shows that the preservation of photoreceptors correlates with a preservation of their synaptic connections (*arrowheads*) with the bipolar cells in retinas from hPi treated animals **(B, D, F)** as compared to control rats **(A, C, E)**. Arrowheads indicate cone photoreceptor contacts. Scale bar: 10 μm.

Discussion

The present study demonstrates that hPi expression attenuates retinal degeneration and the loss of retinal function in P23H rats. Previous studies have already demonstrated the neuroprotective effect of proinsulin (de la Rosa and de Pablo, 2011; de Pablo and de la Rosa, 1995; Vergara *et al.*, 2012), and a recent study showed that transgenic expression of human proinsulin in skeletal muscle in rd10 mice attenuates retinal degeneration (Corrochano *et al.*, 2008). In this work we analyzed the effects of human proinsulin expression on a rat model of autosomal dominant RP characterized by a slow-pace retinal degeneration, the P23H rat (Cuenca *et al.*, 2004; Pinilla *et al.*, 2005). This is the first time that proinsulin therapy has been assayed in this animal model. To express proinsulin in these rats, we used a gene-therapy approach. AAV vectors are becoming the vector of choice for such *in vivo* approaches due to their excellent safety and efficacy profiles. Among several serotypes, the AAV1 is very efficient in transducing the skeletal muscle. High levels of proteins can be secreted into the bloodstream after the injection of this AAV1 into the skeletal muscle (Mas

et al., 2006; Riviere *et al.*, 2006). Preclinical studies have shown that AAV vector–mediated gene transfer results in long-term gene expression in small and large animal models of disease (Mingozzi and High, 2011). Importantly, the European Medicines Agency has recently granted a market authorization for the first gene therapy product in Europe consisting of an AAV1 vector for treating lipoprotein lipase deficiency, which gives support for the potential translation of our approach into the clinic.

In the present study, P23H rats injected intramuscularly with AAV1-hPi vector showed high and consistent levels of proinsulin in the bloodstream (about 1300 pM). The metabolic effects of prolonged systemic exposure to human proinsulin has been extensively investigated in clinical trials, using hPi as an intermediate-acting insulin analog for diabetes therapy (Galloway *et al.*, 1992). Notably, the hypoglycemic potency of proinsulin was ∼5% to 50% that of insulin (Galloway *et al.*, 1969; Jones *et al.*, 1976; Sonksen *et al.*, 1973; Stoll *et al.*, 1971). The serum hPi concentrations, ranging from 1400 to 8000 pM, were equal to or up to 5-fold higher than those achieved in our present study. Importantly, safety studies were performed in patients treated for up to 4 yr with
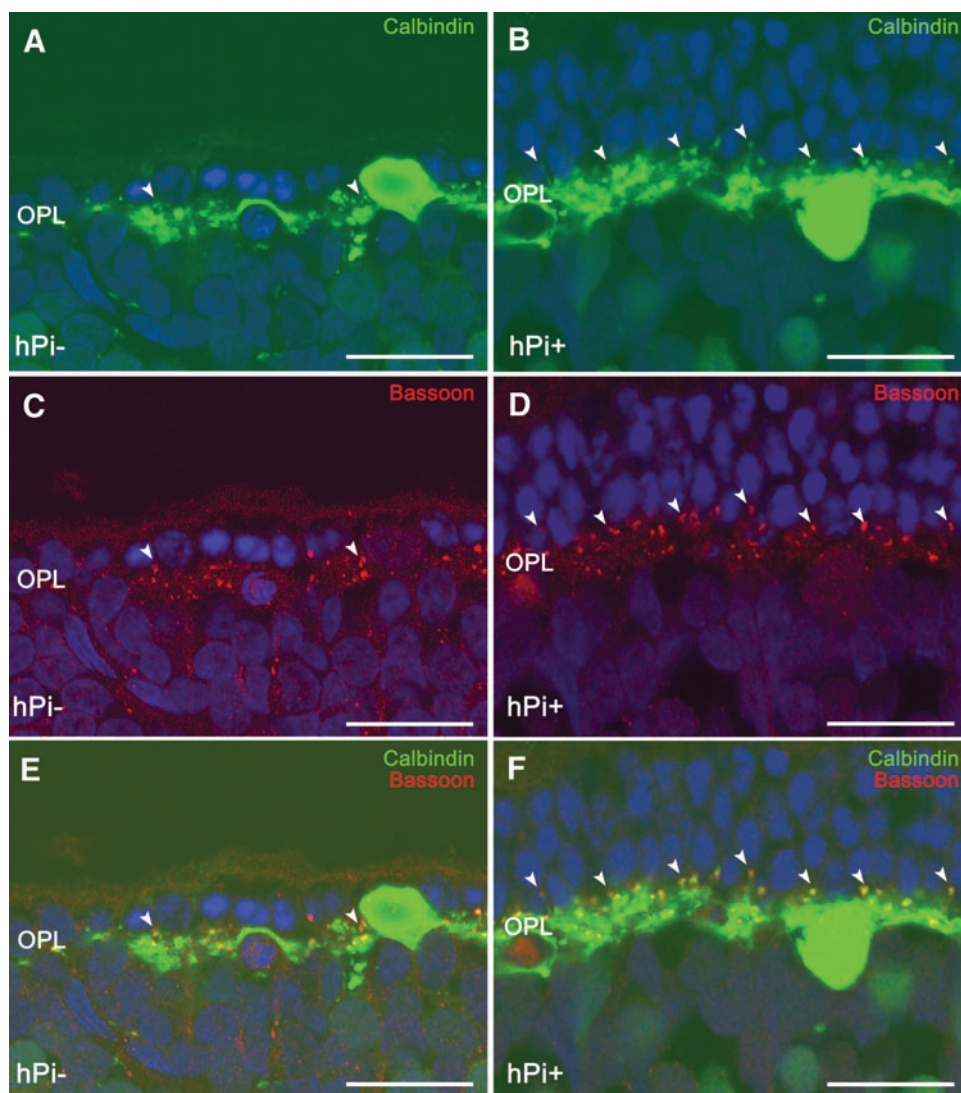
FIG. 6. Horizontal cell synaptic contacts. Immunostaining for calbindin (*green*) and bassoon (*red*) shows a higher number of connections (*arrowheads*) between photoreceptors and horizontal cells in retinas from hPi+ rats **(B, D, F)** than from hPi− animals **(A, C, E)**. Scale bar: 10 μm.

hPi. Compared to insulin, there was no significantly increased risk of retinopathy, arthralgia–arthritis syndromes, or pulmonary embolism (Galloway *et al.*, 1992).

Transgenic P23H rats mimic the clinical findings reported for human patients with P23H RP (Machida *et al.*, 2000; Pinilla *et al.*, 2005). These animals develop a progressive rod dysfunction, albeit initially exhibiting a normal cone function. The loss of photoreceptors is accompanied by degenerative changes in the inner retina (Cuenca *et al.*, 2004), including a substantial degeneration of retinal ganglion cells (Garcia-Ayuso *et al.*, 2010; Kolomiets *et al.*, 2010). P23H line 3 rats retain vision for relatively long periods of their lives, similarly to findings in P23H humans, who exhibit significantly better visual acuity and greater ERG amplitudes than patients harboring other RP mutations (Berson *et al.*, 1991; Machida *et al.*, 2000). The slow retinal degeneration that takes place in P23H line 3 rats makes this animal model closer to the human condition than other P23H lines and genetic mouse models, thus giving the present results additional clinical relevance. In our experiments, proinsulin was detected from P30 to P120, a stage at which P23H animals can be considered to have undergone extensive retinal degeneration

(www.ucsfeye.net/mlavailRDratmodels.shtml; Fernandez-Sanchez *et al.*, 2011; Lax *et al.*, 2011).

Proinsulin expression in P23H rats ameliorated the loss of photoreceptors in these animals. Preservation was in concordance with the higher amplitudes of mixed scotopic ERG responses found in hPi+ animals compared with control animals. These results agree with previous studies carried out in the rd10 retinal degeneration mouse model (Corrochano *et al.*, 2008), in which transgenic hPi/rd10 animals displayed more photoreceptor rows than rd10 animals, and ERG amplitude values of b_{dim}, OP, a_{max}, b_{max}, b_{phot}, and flicker responses were also higher. The greater degree of preservation of photoreceptors and ERG responses observed in hPi/rd10 mice than in the present studies may be attributable to differences in the experimental model. hPi/rd10 mice produces hPi even before birth, while AAV1-hPi–injected P23H rats expressed hPi after P20, when a significant degeneration of both the structure and the visual response of the retina had already occurred (Cuenca *et al.*, 2004; Pinilla *et al.*, 2005). Additionally, the circulating levels of proinsulin in both studies are quite different; in the present work we obtained 100-fold higher levels of circulating

proinsulin (about 1300 pM) compared with the transgenic mice (about 15 pM). In light of these results, we believe that the therapeutic window of proinsulin for RP is very large (and the toxicity threshold is high [Galloway *et al.,* 1992]), since therapeutic effects have been observed at very low doses in rd10 transgenic mouse. At present, while the minimal therapeutic dose of AAV vectors warrants further studies prior to clinical development, we have clearly demonstrated the efficacy of the approach in this proof-of-concept study.

In addition to the preventive effects of hPi on photoreceptor number and function, P23H hPi+ rats demonstrated improved connectivity between photoreceptors and their postsynaptic neurons and horizontal and bipolar cells. Both presynaptic and postsynaptic elements, as well as synaptic contacts between photoreceptors and bipolar or horizontal cells, were preserved in hPi+ rats. Furthermore, the number of rod bipolar cell bodies, as well as the density of their dendritic terminals, was higher in hPi+ than in control rats. These results suggest that the proinsulin effect on retinal morphology and function may not be cell specific and, therefore, may extend not only to photoreceptors but also to other cell types in the retina. On the other hand, preservation of the photoreceptor population may affect the inner retina, preventing the occurrence of secondary degenerative changes in their postsynaptic neurons and subsequent retinal circuitry remodeling.

It has been proposed that neuroprotective effects of proinsulin are exerted, at least in part, through both reducing apoptotic processes and preventing oxidative damage. Blocking antibodies targeting proinsulin induces apoptosis in the early chick retina (Diaz *et al.*, 2000), and treatment with exogenous proinsulin *in ovo* results in a reduction in naturally occurring apoptosis (Hernandez-Sanchez *et al.*, 2003). In the embryonic retina, proinsulin seems to block developmental cell death at various levels, including activation of the prosurvival PI3K/Akt and ERK pathways, stimulation of prosurvival chaperones, and interference with caspases and cathepsins (Chavarria *et al.*, 2007; de la Rosa *et al.*, 1998; Valenciano *et al.*, 2006). Experiments with a rod-specific InsR knockout mouse suggest that reduction of InsR activation could lead to apoptosis mediated by caspase-3 activation (Rajala *et al.*, 2008). Finally, it has been shown that transgenic hPi expression in rd10 mice is able to delay apoptotic death of photoreceptors and to decrease lipid oxidation damage (Corrochano *et al.*, 2008).

In summary the data in this study demonstrate that proinsulin represents a potential new therapy for retinal diseases, and a new tool to characterize the mechanisms involved in pathologic cell death. The use of therapies such as proinsulin, effective not only in preserving photoreceptors from loss but also in slowing the degeneration of inner retinal layers, may be especially interesting in combination with other therapies based on the implantation of new photoreceptors and the use of anti-inflammatory agents, among others.

Author Disclosure Statement

Laura Fernández-Sánchez: F, ProRetina Therapeutics SL. Pedro Lax: F, ProRetina Therapeutics SL. C. Isiegas: I, Pro-Retina Therapeutics SL; E, ProRetina Therapeutics SL. Eduard Ayuso: F, ProRetina Therapeutics SL; I, ProRetina Therapeutics SL. José M. Ruiz: E, ProRetina Therapeutics SL; I, ProRetina Therapeutics SL Pedro de la Villa: F, ProRetina Therapeutics SL; I, ProRetina Therapeutics SL; P, ProRetina Therapeutics SL. Fatima Bosch: F, ProRetina Therapeutics SL; I, ProRetina Therapeutics SL; P, ProRetina Therapeutics SL. Enrique J. de la Rosa: F, ProRetina Therapeutics SL; I, Pro-Retina Therapeutics SL; P, ProRetina Therapeutics SL. Nicolás Cuenca: F, ProRetina Therapeutics SL. F, Financial Support; I, Personal Financial Interest; E, Employment; P, Patent.

References

Ahuja, P., Caffe, A.R., Ahuja, S., *et al.* (2005). Decreased glutathione transferase levels in rd1/rd1 mouse retina: replenishment protects photoreceptors in retinal explants. Neuroscience 131, 935–943.

Ayuso, E., Mingozzi, F., Montane, J., *et al.* (2010). High AAV vector purity results in serotype- and tissue-independent enhancement of transduction efficiency. Gene Ther. 17, 503–510.

Bainbridge, J.W., Smith, A.J., Barker, S.S., *et al.* (2008). Effect of gene therapy on visual function in Leber's congenital amaurosis. N. Engl. J. Med. 358, 2231–2239.

Berson, E.L., Rosner, B., Sandberg, M.A., and Dryja, T.P. (1991). Ocular findings in patients with autosomal dominant retinitis pigmentosa and a rhodopsin gene defect (Pro-23-His). Arch. Ophthalmol. 109, 92–101.

Berson, E.L., Rosner, B., Sandberg, M.A., *et al.* (1993). A randomized trial of vitamin A and vitamin E supplementation for retinitis pigmentosa. Arch. Ophthalmol. 111, 761–772.

Boatright, J.H., Moring, A.G., McElroy, C., *et al.* (2006). Tool from ancient pharmacopoeia prevents vision loss. Mol. Vis. 12, 1706–1714.

Boatright, J.H., Nickerson, J.M., Moring, A.G., and Pardue, M.T. (2009). Bile acids in treatment of ocular disease. J. Ocul. Biol. Dis. Infor. 2, 149–159.

Cayouette, M., Behn, D., Sendtner, M., *et al.* (1998). Intraocular gene transfer of ciliary neurotrophic factor prevents death and increases responsiveness of rod photoreceptors in the retinal degeneration slow mouse. J. Neurosci. 18, 9282–9293.

Cayouette, M., Smith, S.B., Becerra, S.P., and Gravel, C. (1999). Pigment epithelium-derived factor delays the death of photoreceptors in mouse models of inherited retinal degenerations. Neurobiol. Dis. 6, 523–532.

Chadderton, N., Millington-Ward, S., Palfi, A., *et al.* (2009). Improved retinal function in a mouse model of dominant retinitis pigmentosa following AAV-delivered gene therapy. Mol. Ther. 17, 593–599.

Chavarria, T., Valenciano, A.I., Mayordomo, R., *et al.* (2007). Differential, age-dependent MEK-Erk and PI3K-Akt activation by insulin acting as a survival factor during embryonic retinal development. Dev. Neurobiol. 67, 1777–1788.

Chong, N.H., Alexander, R.A., Waters, L., *et al.* (1999). Repeated injections of a ciliary neurotrophic factor analogue leading to long-term photoreceptor survival in hereditary retinal degeneration. Invest. Ophthalmol. Vis. Sci. 40, 1298–1305.

Corrochano, S., Barhoum, R., Boya, P., *et al.* (2008). Attenuation of vision loss and delay in apoptosis of photoreceptors induced by proinsulin in a mouse model of retinitis pigmentosa. Invest. Ophthalmol. Vis. Sci. 49, 4188–4194.

Cuenca, N., Pinilla, I., Sauve, Y., *et al.* (2004). Regressive and reactive changes in the connectivity patterns of rod and cone pathways of P23H transgenic rat retina. Neuroscience 127, 301–317.

de la Rosa, E.J., and de Pablo, F. (2011). Proinsulin: from hormonal precursor to neuroprotective factor. Front. Mol. Neurosci. 4, 20.

de la Rosa, E.J., Vega-Nunez, E., Morales, A.V., *et al.* (1998). Modulation of the chaperone heat shock cognate 70 by embryonic (pro)insulin correlates with prevention of apoptosis. Proc. Natl. Acad. Sci. U. S. A. 95, 9950–9955.

de Pablo, F., and de la Rosa, E.J. (1995). The developing CNS: a scenario for the action of proinsulin, insulin and insulin-like growth factors. Trends Neurosci. 18, 143–150.

Diaz, B., Serna, J., de Pablo, F., and de la Rosa, E.J. (2000). In vivo regulation of cell death by embryonic (pro)insulin and the insulin receptor during early retinal neurogenesis. Development 127, 1641–1649.

Doonan, F., and Cotter, T.G. (2004). Apoptosis: a potential therapeutic target for retinal degenerations. Curr. Neurovasc. Res. 1, 41–53.

Dryja, T.P., McGee, T.L., Reichel, E., *et al.* (1990). A point mutation of the rhodopsin gene in one form of retinitis pigmentosa. Nature 343, 364–366.

Dryja, T.P., McEvoy, J.A., McGee, T.L., and Berson, E.L. (2000). Novel rhodopsin mutations Gly114Val and Gln184Pro in dominant retinitis pigmentosa. Invest. Ophthalmol. Vis. Sci. 41, 3124–3127.

Duenker, N., Valenciano, A.I., Franke, A., *et al.* (2005). Balance of pro-apoptotic transforming growth factor-beta and anti-apoptotic insulin effects in the control of cell death in the postnatal mouse retina. Eur. J. Neurosci. 22, 28–38.

Farrar, G.J., Palfi, A., and O'Reilly, M. (2010). Gene therapeutic approaches for dominant retinopathies. Curr. Gene Ther. 10, 381–388.

Fernandez-Sanchez, L., Lax, P., Pinilla, I., *et al.* (2011). Tauroursodeoxycholic acid prevents retinal degeneration in transgenic P23H rats. Invest. Ophthalmol. Vis. Sci. 52, 4998–5008.

Galloway, J.A., Root, M.A., Chance, R.E., *et al.* (1969). In vivo studies of the hypoglycemic activity of porcine proinsulin. Diabetes 18, 1.

Galloway, J.A., Hooper, S.A., Spradlin, C.T., *et al.* (1992). Biosynthetic human proinsulin. Review of chemistry, in vitro and in vivo receptor binding, animal and human pharmacology studies, and clinical trial experience. Diabetes Care 15, 666–692.

Garcia-Ayuso, D., Salinas-Navarro, M., Agudo, M., *et al.* (2010). Retinal ganglion cell numbers and delayed retinal ganglion cell death in the P23H rat retina. Exp. Eye Res. 91, 800–810.

Green, E.S., Rendahl, K.G., Zhou, S., *et al.* (2001). Two animal models of retinal degeneration are rescued by recombinant adeno-associated virus-mediated production of FGF-5 and FGF-18. Mol. Ther. 3, 507–515.

Hernandez-Sanchez, C, Lopez-Carranza, A., Alarcon, C., *et al.* (1995). Autocrine/paracrine role of insulin-related growth factors in neurogenesis: local expression and effects on cell proliferation and differentiation in retina. Proc. Natl. Acad. Sci. U. S. A. 92, 9834–9838.

Hernandez-Sanchez, C., Mansilla, A., de la Rosa, E.J., *et al.* (2003). Upstream AUGs in embryonic proinsulin mrna control its low translation level. EMBO J. 22, 5582–5592.

Illing, M.E., Rajan, R.S., Bence, N.F., and Kopito, R.R. (2002). A rhodopsin mutant linked to autosomal dominant retinitis pigmentosa is prone to aggregate and interacts with the ubiquitin proteasome system. J. Biol. Chem. 277, 34150–34160.

Jones, B.W., Watt, C.B., Frederick, J.M., *et al.* (2003). Retinal remodeling triggered by photoreceptor degenerations. J. Comp. Neurol. 464, 1–16.

Jones, R.H., Dron, D.I., Ellis, M.J., *et al.* (1976). Biological properties of chemically modified insulins. I. Biological activity of proinsulin and insulin modified at A1-glycine and B29-lysine. Diabetologia 12, 601–608.

Kaushal, S., and Khorana, H.G. (1994). Structure and function in rhodopsin. 7. Point mutations associated with autosomal dominant retinitis pigmentosa. Biochemistry 33, 6121–6128.

Kolomiets, B., Dubus, E., Simonutti, M., *et al.* (2010). Late histological and functional changes in the P23H rat retina after photoreceptor loss. Neurobiol. Dis. 38, 47–58.

Komeima, K., Rogers, B.S., Lu, L., and Campochiaro, P.A. (2006). Antioxidants reduce cone cell death in a model of retinitis pigmentosa. Proc. Natl. Acad. Sci. U. S. A. 103, 11300–11305.

Lax, P., Otalora, B.B., Esquiva, G., *et al.* (2011). Circadian dysfunction in P23H rhodopsin transgenic rats: effects of exogenous melatonin. J. Pineal Res. 50, 183–191.

Liang, F.Q., Aleman, T.S., ZaixinYang, *et al.* (2001). Melatonin delays photoreceptor degeneration in the rds/rds mouse. Neuroreport 12, 1011–1014.

Lock, M., McGorray, S., Auricchio, A., *et al.* (2010). Characterization of a recombinant adeno-associated virus type 2 Reference Standard Material. Hum. Gene Ther. 21, 1273–1285.

Machida, S., Kondo, M., Jamison, J.A., *et al.* (2000). P23H rhodopsin transgenic rat: correlation of retinal function with histopathology. Invest. Ophthalmol. Vis. Sci. 41, 3200–3209.

Maguire, A.M., Simonelli, F., Pierce, E.A., *et al.* (2008). Safety and efficacy of gene transfer for Leber's congenital amaurosis. N. Engl. J. Med. 358, 2240–2248.

Maguire, A.M., High, K.A., Auricchio, A., *et al.* (2009). Age-dependent effects of RPE65 gene therapy for Leber's congenital amaurosis: a phase 1 dose-escalation trial. Lancet 374, 1597–1605.

Marc, R.E., Jones, B.W., Watt, C.B., and Strettoi, E. (2003). Neural remodeling in retinal degeneration. Prog. Retin. Eye Res. 22, 607–655.

Mas, A., Montane, J., Anguela, X.M., *et al.* (2006). Reversal of type 1 diabetes by engineering a glucose sensor in skeletal muscle. Diabetes 55, 1546–1553.

Matsushita, T., Elliger, S., Elliger, C., *et al.* (1998). Adeno-associated virus vectors can be efficiently produced without helper virus. Gene Ther. 5, 938–945.

McGee Sanftner, L.H., Abel, H., Hauswirth, W.W., and Flannery, J.G. (2001). Glial cell line derived neurotrophic factor delays photoreceptor degeneration in a transgenic rat model of retinitis pigmentosa. Mol. Ther. 4, 622–629.

Millington-Ward, S., Chadderton, N., O'Reilly, M., *et al.* (2011). Suppression and replacement gene therapy for autosomal dominant disease in a murine model of dominant retinitis pigmentosa. Mol. Ther. 19, 642–649.

Mingozzi, F., and High, K.A. (2011). Therapeutic in vivo gene transfer for genetic disease using AAV: progress and challenges. Nat. Rev. Genet. 12, 341–355.

Musarella, M.A., and MacDonald, I.M. (2011). Current concepts in the treatment of retinitis pigmentosa. J. Ophthalmol. 2011, 753547.

Okoye, G., Zimmer, J., Sung, J., *et al.* (2003). Increased expression of brain-derived neurotrophic factor preserves retinal function and slows cell death from rhodopsin mutation or oxidative damage. J. Neurosci. 23, 4164–4172.

Palfi, A., Millington-Ward, S., Chadderton, N., *et al.* (2010). Adeno-associated virus-mediated rhodopsin replacement

provides therapeutic benefit in mice with a targeted disruption of the rhodopsin gene. Hum. Gene Ther. 21, 311–323.

Pang, J.J., Dai, X., Boye, S.E., *et al.* (2011). Long-term retinal function and structure rescue using capsid mutant AAV8 vector in the rd10 mouse, a model of recessive retinitis pigmentosa. Mol. Ther. 19, 234–242.

Petterino, C., and Argentino-Storino, A. (2006). Clinical chemistry and haematology historical data in control Sprague-Dawley rats from pre-clinical toxicity studies. Exp. Toxicol. Pathol. 57, 213–219.

Phillips, M.J., Walker, T.A., Choi, H.Y., *et al.* (2008). Tauroursodeoxycholic acid preservation of photoreceptor structure and function in the rd10 mouse through postnatal day 30. Invest. Ophthalmol. Vis. Sci. 49, 2148–2155.

Pinilla, I., Lund, R.D., and Sauve, Y. (2005). Enhanced cone dysfunction in rats homozygous for the P23H rhodopsin mutation. Neurosci. Lett. 382, 16–21.

Pinilla, I., Cuenca, N., Sauve, Y., *et al.* (2007). Preservation of outer retina and its synaptic connectivity following subretinal injections of human Rpe cells in the Royal College of Surgeons rat. Exp. Eye Res. 85, 381–392.

Pinilla, I., Cuenca, N., Martinez-Navarrete, G., *et al.* (2009). Intraretinal processing following photoreceptor rescue by non-retinal cells. Vision Res. 49, 2067–2077.

Puthussery, T., and Taylor, W.R. (2010). Functional changes in inner retinal neurons in animal models of photoreceptor degeneration. Adv. Exp. Med. Biol. 664, 525–532.

Rajala, A., Tanito, M., Le, Y.Z., *et al.* (2008). Loss of neuroprotective survival signal in mice lacking insulin receptor gene in rod photoreceptor cells. J. Biol. Chem. 283, 19781–19792.

Reme, C.E., Grimm, C., Hafezi, F., *et al.* (1998). Apoptotic cell death in retinal degenerations. Prog. Retin. Eye Res. 17, 443–464.

Riviere, C., Danos, O., and Douar, A.M. (2006). Long-term expression and repeated administration of AAV type 1, 2 and 5 vectors in skeletal muscle of immunocompetent adult mice. Gene Ther. 13, 1300–1308.

Sonksen, P.H., Tompkins, C.V., Srivastava, M.C., and Nabarro, J.D. (1973). A comparative study on the metabolism of human insulin and porcine proinsulin in man. Clin. Sci. Mol. Med. 45, 633–654.

Stoll, R.W., Touber, J.L., Winterscheid, L.C., *et al.* (1971). Hypoglycemic activity and immunological half-life of porcine insulin and proinsulin in baboons and swine. Endocrinology 88, 714–717.

Valenciano, A.I., Corrochano, S., de Pablo, F., *et al.* (2006). Proinsulin/insulin is synthesized locally and prevents caspase- and cathepsin-mediated cell death in the embryonic mouse retina. J. Neurochem. 99, 524–536.

Vergara, M.N., de la Rosa, E.J., and Canto-Soler, M.V. (2012). Focus on molecules: proinsulin in the eye: precursor or pioneer? Exp. Eye Res. 101, 109–110.

Address correspondence to:
Dr. Nicolás Cuenca
Departamento de Fisiología, Genética y Microbiología
Universidad de Alicante
Campus Universitario San Vicente
Apartado 99
E-03080 Alicante
Spain

E-mail: cuenca@ua.es